Article:

Lamberto, G. orcid.org/0000-0001-7038-2655, Richard, V., Dumas, R. et al. (5 more authors) (2016) Modeling the human tibio-femoral joint using ex vivo determined compliance matrices. Journal Of Biomechanical Engineering, 138 (6). 061010. ISSN 0148-0731

https://doi.org/10.1115/1.4033480

Modeling the human tibio-femoral joint using ex vivo determined compliance matrices

Giuliano Lamberto[1]
Department of Movement, Human, and Health Sciences
Università degli Studi di Roma - Foro Italico
Piazza Lauro de Bosis 6
00194 Rome, Italy
Department of Mechanical Engineering and INSIGNEO Institute for *in silico* Medicine,
University of Sheffield,
Mappin Street,
Sheffield - S1 3JD, United Kingdom
e-mail: glamberto1@sheffied.ac.uk

Vincent Richard
Universite´ de Lyon,
Universite´ Claude Bernard Lyon 1, IFSTTAR, UMR_T9406
Laboratoire de Biomécanique et Mécanique des Chocs
Bron, France
e-mail: vincent.richard@univ-lyon1.fr

Raphaël Dumas
Universite´ de Lyon,
Universite´ Claude Bernard Lyon 1, IFSTTAR, UMR_T9406
Laboratoire de Biomécanique et Mécanique des Chocs
Bron, France
e-mail: raphael.dumas@ifsttar.fr

Pier Paolo Valentini
Department of Enterprise Engineering "Mario Lucertini"
Università degli Studi di Roma - Tor Vergata
Via del Politecnico, 1
00133 Rome, Italy
e-mail: valentini@ing.uniroma2.it

[1] Corresponding author at: Department of Mechanical Engineering, The University of Sheffield, INSIGNEO Institute for in silico medicine, Room C+ 13, C+ floor, The Pam Liversidge Building, Sir Frederick Mappin Building, Mappin Street, Sheffield - S1 3JD, UK. E-mail address: glamberto1@sheffield.ac.uk

Ettore Pennestrì
Department of Enterprise Engineering “Mario Lucertini”
Università degli Studi di Roma - Tor Vergata
Via del Politecnico, 1
00133 Rome, Italy
e-mail: pennestri@mec.uniroma2.it
ASME Member

Tung-Wu Lu
Institute of Biomedical Engineering, and
Department of Orthopedic Surgery
National Taiwan University
No. 1, Section 4, Roosevelt Road
Taipei 106, Taiwan
e-mail: twlu@ntu.edu.tw

Valentina Camomilla
Department of Movement, Human, and Health Sciences
Università degli Studi di Roma - Foro Italico
Piazza Lauro de Bosis 6
00194 Rome, Italy
e-mail: valentina.camomilla@uniroma4.it

Aurelio Cappozzo
Department of Movement, Human, and Health Sciences
Università degli Studi di Roma - Foro Italico
Piazza Lauro de Bosis 6
00194 Rome, Italy
e-mail: aurelio.cappozzo@uniroma4.it

ABSTRACT

Several approaches have been used to devise a model of the human tibio-femoral joint for embedment in lower limb musculoskeletal models. However, no study has considered the use of cadaveric 6x6 compliance (or stiffness) matrices to model the tibio-femoral joint under normal or pathological conditions. The aim of this paper is to present a method to determine the compliance matrix of an ex vivo tibio-femoral joint for any given equilibrium pose. Experiments were carried out on a single ex vivo knee, first intact and, then, with the anterior cruciate ligament (ACL) transected. Controlled linear and angular displacements were imposed in single degree-of-freedom (DoF) tests to the specimen and resulting forces and moments measured using an instrumented robotic arm. This was done starting from seven equilibrium poses characterized by the following flexion angles: 0°, 15°, 30°, 45°, 60°, 75°and 90°. A compliance matrix for each of the selected equilibrium poses and for both the intact and ACL deficient specimen was calculated. The matrix, embedding the experimental load-displacement relationship of the examined DoFs, was calculated using a linear least squares inversion based on a QR decomposition, assuming symmetric and positive-defined matrices. Single compliance matrix terms were in agreement with the literature. Results showed an overall increase of the compliance matrix terms due to the ACL transection (2.6 ratio for rotational terms at full extension) confirming its role in the joint stabilization. Validation experiments were carried out by performing a Lachman test (the tibia is pulled forward) under load control on both the intact and ACL-deficient knee and assessing the difference (error) between measured linear and angular displacements and those estimated using the appropriate compliance matrix. This error increased non-linearly with respect to the values of the load. In particular, when an incremental posterior-anterior force up to 6 N was applied to the tibia of the intact specimen, the errors on the estimated linear and angular displacements were up to 0.6 mm and 1.5°, while for a force up to 18 N the errors were 1.5 mm and 10.5°, respectively.

In conclusion, the method used in this study may be a viable alternative to characterize the tibio-femoral load-dependent behavior in several applications.

INTRODUCTION

Biomechanical modeling of the knee joint has been the object of several studies in the last 30 years [1–12] with the aim of better understanding the passive joint behavior and estimate the joint contact and ligament forces during motor tasks under physiological and pathological conditions. To address these objectives, comprehensive finite element or multi-body models [13–18] have been developed and, in some cases, validated against *ex vivo* data. Due to numerical issues, knee models in general rely on kinematic constraints (i.e. degree-of-freedom (DoF) restraints) [8,19], which may include ligaments with infinite stiffness and/or passive joint moments [20,21]. The passive joint moments are linear or exponential functions of the joint angles and are introduced in simulations mainly with the aim of preventing exceedingly large joint amplitudes. The stiffness values, embedded in these curves, are not determined experimentally but result from a tuning or calibration procedure and comply with numerical requirements of the optimization approach. Another modeling approach, called "force dependent kinematics", has been recently proposed [22,23]. The idea is to optimize the estimate of joint kinematics to ensure the static equilibrium of the joint according to a set of stiffness values, again, resulting from a numerical procedure.

An alternative modeling approach would be to directly introduce a knee compliance matrix (or its inverse named stiffness matrix) resulting from ex vivo experiments into the musculoskeletal model. This matrix provides the joint displacements as a function of the loads acting through the joint. Such approach has been previously proposed for the intervertebral joints [24–27], but not for other joints. One interesting property of the compliance matrix is that the extra-diagonal terms describe the physiological couplings between the DoFs. In addition, pathological conditions, such as ligament or meniscal tears, can be revealed by altered matrix terms. Nevertheless, despite a general availability of robotic-manipulators [28], the knowledge of the knee compliance matrix is rather limited. Indeed, investigations of the tibio-femoral joint kinematics response to loading have been restricted either to few selected directions or to a limited number of knee configurations (i.e., typically 0° of flexion). For example, Markolf et al. [29] performed one of the most complete studies available, analyzing the relationship between moments and adduction-abduction and internal-external rotations, as well as force and linear displacement in the anterior-posterior direction, at six different flexion angles. Eagar et al. [30] quantified the anterior-posterior load-displacement behavior in both linear and non-linear regions at four different flexion angles. Fox et al. [31] and Kanamori et al. [32] determined the *in situ* forces in the posterior and anterior cruciate ligaments, respectively, in response to different loading conditions and in more than one configuration (i.e. 0°, 15°, 30°, 60°, 90° of flexion). However, to the best of our knowledge, only Loch et al. [33] tried to characterize the mechanical behavior of the passive structures that constrain the knee joint using a compact 6x6 matrix, but that research was limited to a single knee configuration (i.e., 0° of flexion). Moreover, the way the terms of the matrix were derived from experimental data is not clearly stated.

The aim of this paper was to present a method to mathematically define and experimentally determine a set of compliance matrices in different knee configurations. The current study used a quasi-static approach by applying, through a robotic arm, small displacements about a number of selected equilibrium poses of the knee [31,32]. The load-displacement relationships were expressed by 6x6 symmetric compliance matrices. Experiments were carried out on a cadaveric knee specimen, both intact and with the anterior cruciate ligament (ACL) transected. In addition, a validation procedure was implemented to test the ability of the compliance matrix to estimate linear and angular displacements as caused by an arbitrary load.

MATERIALS AND METHODS

Specimen preparation

A single intact fresh-frozen human knee joint obtained from a 75 year old female was tested. The specimen was a left leg derived from an amputation due to an acute arterial occlusion. Ethical approval for the study was granted by the Institutional Research Board of China Medical University Hospital (Taichung City, Taiwan). The knee was kept frozen until the time of use. It was declared normal by the surgeon who prepared it for the experiments. It was sectioned at the mid-shaft of the femur and tibia and dissected down to the joint capsule and major ligaments. All the muscles, the patella, and the patellar tendon were removed in order to mechanically characterize the behavior of the tibio-femoral passive structures. The bones were mounted through cement in two aluminum fixation supports to be connected to a Robot-based Joint Testing System (RJTS) [34]. On the day of testing, the knee was thawed and pre-conditioned [35]. After testing the intact knee, all the ACL bundles were surgically transected and the experimental procedure repeated.

Experimental apparatus and procedure

The RJTS consists of an industrial robotic system (RV-20A, Mitsubishi Electric Corporation, Japan) and a six-component load cell (Universal Force Sensor, Model PY6-100, Bertec Corporation, USA) that was attached to the end effector of the robot for the measurement of the three force and three moment components of the load (Figure 1A). The robot was recently developed for applications in *ex vivo* biomechanical studies [34]. This testing device is capable of a hybrid position/load control using traditional and innovative methods. Control methods were evaluated performing tests on a human cadaveric knee both in translation along and in rotation about a selected axis, where their convergence and their residual constraining load were compared against published standard methods. The results, showing a repeat accuracy of 0.1 mm, suggested system suitability for accurate and reliable testing of biological joints [34]. The sampling rate of the acquisition was 10 samples per second.

A method to identify bony landmarks for the definition of femur and tibia anatomical coordinated systems and therefore of the knee joint coordinate system (JCS) was adapted from Fujie et al. [36] (Figure 1A). A calibration procedure was performed using a pointer mounted on the end-effector of the robot. Using this pointer, the position of the femoral insertion sites of the medial collateral ligament and the lateral collateral ligament were identified in the global coordinate system. The centroid of the femoral section was assumed as coincident with the geometrical center of the fixation support, the position of which was determined before mounting the specimen. These points were used to define the anatomical coordinate system of the femur (C_f) (details in Figure 1B). The anatomical coordinate system of the tibia (C_t) was defined as coincident with C_f at full extension. The forces and moments were recorded by the load cell in the sensor coordinate system (C_s) (Figure 1A).

Flexion-extension (F-E), adduction-abduction (A-A), and internal-external (I-E) rotations were defined as motions about the JCS axes (e1: *z*-axis of C_f, e2: floating axis, e3: y-axis of C_t). Medial-lateral (M-L), anterior-posterior (A-P), and proximal-distal (P-D) linear displacements were characterized as motions along these axes. A sign inversion was used to report positive values for the flexion angles, otherwise negative by convention. Measured loads were represented in the JCS using a Jacobian matrix [37].

A set of pre-determined F-E angles were used to determine the compliance matrices of the intact knee: 0°, 15°, 30°, 45°, 60°, 75°and 90°. For each F-E angle, the neutral pose, i.e. the A-A and I-E rotations, and M-L, A-P and P-D displacements, was determined so that the measured joint moments and forces were minimal [37]. The same neutral poses were later used for the ACL-deficient knee experiment. Constrained control was then used to perform single DoF tests [34]. These tests were defined by the application of the following procedure: starting from the neutral pose, linear or angular displacement increments (at rates of 0.93 mm/s and 0.97 °/s) were applied one at a time along and about each single DoF, under moment and force limitations to avoid any damage to the soft tissues. The force limitations, adopted both for the intact and ACL-deficient knee, were 100 N along A-P and P-D, and 80 N along L-M as similarly applied in [38]. Limitations of moments were conservatively set at 25% of those used in [29,39], and were 2.5 Nm for A-A, and 1 Nm for I-E.

To evaluate the prediction capability of the compliance matrix, a Lachman test was simulated. With the knee flexed at 30°, a force, linearly increasing in time, was applied to the tibia along the A-P axis, under the force limitation mentioned previously. The whole experimental procedure is summarized in Table 1.

Post-processing procedure

The post-processing procedure was based on the procedure proposed by Stokes et al. [40] and adapted to the experimental data of the present study.

The compliance matrix $[C]$ is 6x6 symmetric:

$$[C]\{F - F_0\} = \{X - X_0\} \tag{1}$$

where $\{X\}$ is a 6x1 generalized displacement vector of the A-P, P-D and M-L displacements followed by the A-A, I-E, and F-E rotations and $\{F\}$ is a 6x1 load vector of the corresponding forces and moments. $\{X_0\}$ and $\{F_0\}$ are the same 6x1 vectors obtained at the neutral poses of the knee. The generic 6x6 symmetric compliance matrix

[C] has 21 independent compliance terms (6 translational, 6 rotational, and 9 coupling terms), $\{c\}$, that can be obtained by rearranging Eq. 1 into the standard least squares inversion form:

$$[L]\{c\} = \{X - X_0\} \tag{2}$$

where $[L]$ is a 6x21 matrix based on the six terms of $\{F - F_0\}$ (the incremental load vectors) and $\{c\}$ is a 21x1 vector of the 21 independent compliance matrix terms. This vector $\{c\}$ was obtained through a least squares inversion using, for each F-E angle, the 3D displacements and loads obtained from all the incremental displacements applied about each single DoF. In this way, it is not the 6*6 matrix terms that were computed but the 21 independent terms directly. Thus, the 9 coupling terms have not been averaged to make the matrix symmetric, as is performed classically in the literature [41]. Compliance terms were set as unknown to be determined with respect to the stiffness terms. This approach prevented proportional vectors in the coefficient matrix of the standard least squares form (Eq. 2). In fact, setting stiffness terms as unknown would have filled the coefficient matrix with the proportional imposed linear increments of the single DoF tests, introducing a rank-deficiency in the computation. In addition, a QR decomposition was used to avoid numerical instability [42] and each matrix was constrained to be positive defined. Re-sampling using cubic spline interpolation was performed since the data has different frame numbers, according to the different moment and force limitations imposed. Ultimately, only the first fifteen frames were considered to ensure a certain range of linearity around the neutral pose and, at the same time, to consider the contribution of each single DoF test to the overall matrix. Concerning the latter aspect, at least ten frames from each single DoF test were assumed to be representative in the overall matrix.

Validation

For the purpose of validation, the compliance matrices computed at 30° of F-E with both intact and ACL-deficient knee were used to predict the A-P, P-D and M-L displacements and A-A, I-E and F-E rotations using Eq. 1 and the forces and moments measured during the simulated Lachman test. The absolute errors between calculated and measured linear and angular displacements were computed.

RESULTS

The compliance matrices for the intact and the ACL-deficient knee are displayed at 0° and 30° of F-E in Table 2 and Table 3, respectively. The matrices for the other neutral poses can be found in the Appendix.

The vast majority of the calculated compliance terms were modified by the ACL transection. As expected, the values of the compliance terms increased after the ACL dissection when compared to their values for the intact knee structures. For instance, at full extension, the incremental ratios between the sum of the compliance terms of each subgroup before and after the dissection were 1.51, 2.60, and 0.83 for the translational, rotational, and coupling terms, respectively. This behavior accounts for the fundamental role of the ACL in preventing extreme tibio-femoral displacements when a force is applied. In addition, non-negligible coupling terms depending to the particular flexion angle were found. This highlights the fact that it is important to estimate the compliance matrix in more than one configuration.

The validation tests performed using the compliance matrices obtained at 30° of F-E for the intact and ACL-deficient knee (Table 3), are illustrated in Figure 2 and Figure 3, respectively. The following quantities are depicted as a function of time: the absolute errors (panels A and B) and the values of the three linear and three angular displacement components (panels C and D) computed through the compliance matrix (Eq. 1) using the forces and moments (panels E and F) recorded during the simulated Lachman test. Coherent results were achieved both for the intact and the ACL-deficient knees at the beginning of the validation experiments, that is, when small loads were applied in proximity of the neutral pose. However, at a later stage of the experiment, absolute errors were found to increase. In particular, for controlled forces below 6 N and 3 N for the intact and the ACL-deficient knee (0-0.5 s of testing), the maximum absolute errors were 0.58 mm, 0.21 mm and 1.49°, 0.57° for the linear and angular displacements, respectively. For controlled forces below 11 N and 8 N (0.6-1 s of testing), the errors were 1.14 mm, 0.83 mm, and 4.60°, 2.95°, respectively and increased to 1.49 mm, 2.35 mm, and 10.36°, 3.36° when forces reached 18 N and 15 N (1.1-1.5 s of testing).

DISCUSSION

In the present study, the mathematical definition and experimental determination of compliance matrices in different knee configurations was developed.

The mathematical definition is based on a compliance matrix which led to a higher number of independent rows in the calculation process with respect to the stiffness matrix. The compliance terms are computed through a least squares inversion based on QR decomposition, and the positive definition of all the matrices computed was ensured for a possible use as stiffness matrices. The experimental determination was performed, using a previously described Robot-based Joint Testing System [34], in different knee configurations on both an intact and ACL-deficient knee. The compliance of the knee/robot complex was computed under the assumption that the stiffness of the robot components is much higher than the knee surrounding tissues and, therefore, can be attributed exclusively to the knee [31,39].

Validation tests of the compliance matrix determined at 30° of F-E (Lachman test) confirmed the ability to predict the A-P, P-D and M-L displacements and A-A, I-E and F-E rotations for given loads applied on the JCS axes. The maximum absolute error between predicted and measured knee linear and angular displacements increased non-linearly with respect to the values of the applied load, both for the intact and the ACL-deficient knee. As a result of the deviations from the starting neutral pose (more than 1mm and/or 1°) occurring when a force higher than 10 N in the A-P direction was applied, caution should be exercised in using the compliance matrix when high loads/displacements occur. This is also why only the first fifteen frames of the linear and angular increments of each single DoF test were used for the determination of the compliance terms. Some preliminary tests revealed that for a larger number of frames the residual of the least squares inversion was higher. The cited number of frames was selected as a good trade-off between a warranted linearity of load-displacement curves and an ensured contribution of each single DoF test to the overall matrix.

Although no other study performed the determination of a set of compliance matrices in different knee configurations, the current results can be compared with studies estimating specific terms of the compliance matrix obtained at 0° of F-E (Table 2). The obtained compliance terms in the first row and first column compared well with those obtained in *Markolf*'s work [29], during an A-P stability test: the ratio after and before ACL-section was 0.29 in the current study and 0.31 in [29]. Similarly, in A-P direction the first diagonal term (about 0.08 mm/N) was in the range obtained by Eagar et al. [30] who tested seven intact knee specimens (between 0.02 and 0.17 mm/N). However, in that study, the neutral path of flexion-extension at the knee was not defined and, as a result, no other knee configuration can be compared with the current study. Ultimately, comparing our results with the stiffness matrix calculated by Loch et al. [33] some similarities and differences could be found. In particular, the first two translation compliance terms have the same order of magnitude as in [33], during six independent displacement tests. Conversely, in our compliance matrix the third translation compliance term and the rotational terms are two or more orders of magnitude bigger than in [33]. These discrepancies can be attributed to the difference in the neutral pose at full extension since a preload was applied in [33].

The current study is based on one important assumption, which may limit the domain of application of the obtained results. In accordance with the literature [33], it is assumed that, for small linear or angular displacements relative to the overall dimension of the knee bones, the load-displacement behavior is linear, i.e. the compliance matrices are symmetric. A second limiting factor in the application of current results is narrowing the focus only on the passive structures that constrain the human knee, therefore excluding muscular tendinous tissues, patella and patellar tendon as possible contributors to the stability or load-bearing forces. Thirdly, this study focused on only one knee specimen as other studies did [43,44]. The experimental procedure was extremely time-consuming and the focus was more on determining the compliance matrices in different knee configurations than testing multiple specimens.

Despite the limitations mentioned, the proposed set of compliance matrices can be used to model the knee joint for its effective embedment in a musculoskeletal model of the lower limb with low computational cost. The stiffness matrix (i.e., inverse of the compliance matrix) of the intervertebral joints has been widely used in multi-body models [24,26,45,46]. The study proposed here for the knee joint could be the first step on the path covered previously for the spine. For that, the definition of the neutral pose is of paramount importance to compute the joint passive moments and the elastic energy. As shown in the compliance matrix validation performed in the current study, this joint modeling is valid only near the neutral poses. Therefore, the definition of a set of compliance matrices at different knee configurations (0°, 15°, 30°, 45°, 60°, 75° and 90° in this work) is of paramount importance.

The introduction of these matrices, or of corresponding stiffness matrices, into musculoskeletal models of the lower limb will be the next step to provide alternatives for femur and tibia pose estimation during movement using stereophotogrammetry and skin markers and the so-named multi-body optimization [47]. Such “compliant” constraints may provide better results than infinitely stiff constraints, like spherical or hinge joints or parallel mechanisms [48–50]. The use of the matrices determined with the ACL-deficient knee open the way for defining pathological constraints.

In conclusion, the method proposed in this study may be a viable alternative to characterize the tibio-femoral load-dependent behavior in several applications. This contribution might have implications on a new generation of lower limb musculoskeletal models.

ACKNOWLEDGMENT

The authors wish to thank Li-De Chang, Tchung Whao, Mei-Ying Kuo, Elena Bergamini and Valerio Rossi for providing technical and logistical support during and after the experimental tests of this research.

FUNDING

This study was supported by a grant provided by the Università di Roma “Foro Italico”, call 2012, named “A piecewise elastic model of the human tibiofemoral joint: a feasibility study”.

APPENDIX

Compliance matrices at 15°, 45°, 60°, 75° and 90° of F-E for both intact and ACL-sectioned knee tested are shown in Table 4 and Table 5.

REFERENCES

[1] Yamaguchi, G. T., and Zajac, F. E., 1989, “A planar model of the knee joint to characterize the knee extensor mechanism,” J. Biomech., **22**(1), pp. 1–10.

[2] Beynnon, B., Yu, J., Huston, D., Fleming, B., Johnson, R., Haugh, L., and Pope, M. H., 1996, “A sagittal plane model of the knee and cruciate ligaments with application of a sensitivity analysis.,” J. Biomech. Eng., **118**(2), pp. 227–39.

[3] Hu, C.-C., Lu, T.-W., and Chen, S.-C., 2013, “Influence of model complexity and problem formulation on the forces in the knee calculated using optimization methods.,” Biomed. Eng. Online, **12**(1), p. 20.

[4] Fernandez, J. W., and Pandy, M. G., 2006, “Integrating modelling and experiments to assess dynamic musculoskeletal function in humans.,” Exp. Physiol., **91**(2), pp. 371–82.

[5] Yang, N. H., Canavan, P. K., Nayeb-Hashemi, H., Najafi, B., and Vaziri, A., 2010, “Protocol for constructing subject-specific biomechanical models of knee joint.,” Comput. Methods Biomech. Biomed. Engin., **13**(5), pp. 589–603.

[6] Halloran, J. P., Petrella, A. J., and Rullkoetter, P. J., 2005, “Explicit finite element modeling of total knee replacement mechanics.,” J. Biomech., **38**(2), pp. 323–31.

[7] Ribeiro, A., Rasmussen, J., Flores, P., and Silva, L. F., 2012, “Modeling of the condyle elements within a biomechanical knee model,” Multibody Syst. Dyn., **28**(1-2), pp. 181–197.

[8] Arnold, E. M., Ward, S. R., Lieber, R. L., and Delp, S. L., 2010, “A model of the lower limb for analysis of human movement.,” Ann. Biomed. Eng., **38**(2), pp. 269–79.

[9] Sancisi, N., and Parenti-Castelli, V., 2011, “A sequentially-defined stiffness model of the knee,” Mech. Mach. Theory, **46**(12), pp. 1920–1928.

[10] Baldwin, M. a, Clary, C. W., Fitzpatrick, C. K., Deacy, J. S., Maletsky, L. P., and Rullkoetter, P. J., 2012, “Dynamic finite element knee simulation for evaluation of knee replacement mechanics.,” J. Biomech., **45**(3), pp. 474–83.

[11] Shelburne, K. B., Torry, M. R., and Pandy, M. G., 2005, “Muscle, Ligament, and Joint-Contact Forces at the Knee during Walking,” Med. Sci. Sport. Exerc., **37**(11), pp. 1948–1956.

[12] Moissenet, F., Chèze, L., and Dumas, R., 2014, “A 3D lower limb musculoskeletal model for simultaneous estimation of musculo-tendon, joint contact, ligament and bone forces during gait.,” J. Biomech., **47**(1), pp. 50–8.

[13] Bendjaballah, M. Z., Shirazi-Adl, a., and Zukor, D. J., 1998, “Biomechanical response of the passive human knee joint under anterior-posterior forces.,” Clin. Biomech. (Bristol, Avon), **13**(8), pp. 625–633.

[14] Donahue, T. L. H., Hull, M. L., Rashid, M. M., and Jacobs, C. R., 2002, “A finite element model of the human knee joint for the study of tibio-femoral contact.,” J. Biomech. Eng., **124**(3), pp. 273–80.

[15] Peña, E., Calvo, B., Martínez, M. a, and Doblaré, M., 2006, “A three-dimensional finite element analysis of the combined behavior of ligaments and menisci in the healthy human knee joint.,” J. Biomech., **39**(9), pp. 1686–701.

[16] Li, G., Gil, J., Kanamori, a, and Woo, S. L., 1999, “A validated three-dimensional computational model of a human knee joint.,” J. Biomech. Eng., **121**(6), pp. 657–62.

[17] Guess, T. M., Thiagarajan, G., Kia, M., and Mishra, M., 2010, “A subject specific multibody model of the knee with menisci.,” Med. Eng. Phys., **32**(5), pp. 505–15.

[18] Kazemi, M., Dabiri, Y., and Li, L. P., 2013, “Recent advances in computational mechanics of the human knee joint.,” Comput. Math. Methods Med., **2013**, p. 718423.

[19] Xu, H., Bloswick, D., and Merryweather, A., 2014, “An improved OpenSim gait model with multiple degrees of freedom knee joint and knee ligaments.,” Comput. Methods Biomech. Biomed. Engin., **18**(11), pp. 1217–1224.

[20] Al Nazer, R., Rantalainen, T., Heinonen, a, Sievänen, H., and Mikkola, a, 2008, “Flexible multibody simulation approach in the analysis of tibial strain during walking.,” J. Biomech., **41**(5), pp. 1036–43.

[21] Anderson, F. C., and Pandy, M. G., 2001, “Dynamic Optimization of Human Walking,” J. Biomech. Eng., **123**(5), pp. 381–390.

[22] Andersen, M., Damsgaard, M., and Rasmussen, J., 2011, “Force-dependent kinematics: a new analysis method for non-conforming joints,” 13th International Symposium on Computer Simulation in Biomechanics, pp. 1–2.

[23] Andersen, M., and Rasmussen, J., 2011, “Total knee replacement musculoskeletal model using a novel simulation method for non-conforming joints,” Proceedings of the International Society of Biomechanicsof the International Society of Biomechanics, pp. 1–2.

[24] Christophy, M., Faruk Senan, N. A., Lotz, J. C., and O’Reilly, O. M., 2012, “A Musculoskeletal model for the lumbar spine,” Biomech. Model. Mechanobiol., **11**(1), pp. 19–34.

[25] Koell, P., Cheze, L., and Dumas, R., 2010, “Prediction of internal spine configuration from external measurements using a multi-body model of the spine,” Comput. Methods Biomech. Biomed. Engin., **13**(sup1), pp. 79–80.

[26] Petit, Y., Aubin, C. E., and Labelle, H., 2004, “Patient-specific mechanical properties of a flexible multi-body model of the scoliotic spine,” Med. Biol. Eng. Comput., **42**(1), pp. 55–60.

[27] Marin, F., Hoang, N., Aufaure, P., and Ho Ba Tho, M. C., 2010, “In vivo intersegmental motion of the cervical spine using an inverse kinematics procedure,” Clin. Biomech., **25**(5), pp. 389–396.

[28] Fujie, H., Mabuchi, K., and Woo, S., 1993, “The use of robotics technology to study human joint kinematics: a new methodology.,” J. Biomech. Eng., **115**(3), pp. 211–7.

[29] Markolf KL, Mensch, J., and Amstutz, H., 1976, “Stiffness and laxity of the knee - the contributions of the supporting structures.,” J. Bone Joint Surg. Am., **58**(5), pp. 583–94.

[30] Eagar, P., Hull, M. L., and Howell, S. M., 2001, “A method for quantifying the anterior load-displacement behavior of the human knee in both the low and high stiffness regions.,” J. Biomech., **34**(12), pp. 1655–60.

[31] Fox, R. J., Harner, C. D., Sakane, M., Carlin, G. J., and Woo, S. L., 1998, “Determination of the in situ forces in the human posterior cruciate ligament using robotic technology. A cadaveric study.,” Am. J. Sports Med., **26**(3), pp. 395–401.

[32] Kanamori, A., Woo, S. L., Ma, C. B., Zeminski, J., Rudy, T. W., Li, G., and Livesay, G. a, 2000, “The forces in the anterior cruciate ligament and knee kinematics during a simulated pivot shift test: A human cadaveric study using robotic technology.,” Arthroscopy, **16**(6), pp. 633–9.

[33] Loch, D. a, Luo, Z. P., Lewis, J. L., and Stewart, N. J., 1992, “A theoretical model of the knee and ACL: theory and experimental verification.,” J. Biomech., **25**(1), pp. 81–90.

[34] Hsieh, H.-J., Hu, C.-C., Lu, T.-W., Kuo, M.-Y., Kuo, C.-C., and Hsu, H.-C., “Evaluation of Three Force-Position Hybrid Control Methods for a Robot-Based Biological Joint Testing System,” Submitt. to Biomed. Eng. Online.

[35] Most, E., Axe, J., Rubash, H., and Li, G., 2004, “Sensitivity of the knee joint kinematics calculation to selection of flexion axes.,” J. Biomech., **37**(11), pp. 1743–8.

[36] Fujie, H., Sekito, T., and Orita, A., 2004, “A novel robotic system for joint biomechanical tests: application to the human knee joint.,” J. Biomech. Eng., **126**(1), pp. 54–61.

[37] Fujie, H., Livesay, G., Fujita, M., and Woo, S., 1996, “Forces and moments in six-DOF at the human knee joint: mathematical description for control,” J. Biomech., **29**(12), pp. 1577–1585.

[38] Grood, E., 1988, “Limits of movement in the human knee. Effect of sectioning the posterior cruciate ligament and posterolateral structures,” J Bone Jt. Surg Am, pp. 88–97.

[39] Zantop, T., Herbort, M., Raschke, M. J., Fu, F. H., and Petersen, W., 2007, “The role of the anteromedial and posterolateral bundles of the anterior cruciate ligament in anterior tibial translation and internal rotation.,” Am. J. Sports Med., **35**(2), pp. 223–7.

[40] Stokes, I. a, Gardner-Morse, M., Churchill, D., and Laible, J. P., 2002, “Measurement of a spinal motion segment stiffness matrix.,” J. Biomech., **35**(4), pp. 517–21.

[41] Gardner-Morse, M. G., and Stokes, I. a. F., 2004, “Structural behavior of human lumbar spinal motion segments,” J. Biomech., **37**(2), pp. 205–212.

[42] Pennestrì, E., and Cheli, F., 2006, Cinematica e dinamica dei sistemi multibody (in italian), vol.1, Casa Editrice Ambrosiana, Milano, Italy.

[43] Guess, T. M., Liu, H., Bhashyam, S., and Thiagarajan, G., 2011, “A multibody knee model with discrete cartilage prediction of tibio-femoral contact mechanics.,” Comput. Methods Biomech. Biomed. Engin., **16**(3), pp. 256–70.

[44] Mommersteeg, T. J., Huiskes, R., Blankevoort, L., Kooloos, J. G., and Kauer, J. M., 1997, “An inverse dynamics modeling approach to determine the restraining function of human knee ligament bundles.,” J. Biomech., **30**(2), pp. 139–46.

[45] Christophy, M., Curtin, M., Faruk Senan, N. A., Lotz, J. C., and O’Reilly, O. M., 2013, “On the modeling of the intervertebral joint in multibody models for the spine,” Multibody Syst. Dyn., **30**, pp. 413–432.

[46] Kim, K., Kim, Y. H., and Lee, S., 2012, “General computational model for human musculoskeletal system of spine,” J. Appl. Math., **2012**, pp. 1–8.

[47] Lu, T.-W., and O’Connor, J. J., 1999, “Bone position estimation from skin marker co-ordinates using global optimisation with joint constraints,” J. Biomech., **32**(2), pp. 129–134.

[48] Mokhtarzadeh, H., Perraton, L., Fok, L., Muñoz, M. A., Clark, R., Pivonka, P., and Bryant, A. L., 2014, “A comparison of optimisation methods and knee joint degrees of freedom on muscle force predictions during single-leg hop landings.,” J. Biomech., **47**(12), pp. 2863–2868.

[49] Di Gregorio, R., and Parenti-Castelli, V., 2003, “A Spatial Mechanism With Higher Pairs for Modelling the Human Knee Joint,” J. Biomech. Eng., **125**(2), pp. 232–7.

[50] Ottoboni A, Parenti-Castelli V, Sancisi N, Belvedere C, L. A., 2010, “Articular surface approximation in equivalent spatial parallel mechanism models of the human knee joint: an experiment-based assessment.,” Proc Inst Mech Eng H.

Figure Captions List

Fig. 1 A) A schematic representation of the Robot-based Joint Testing System (RJTS) and the reference systems used are provided: G is the global coordinate system; C_s is the coordinate system of the load cell (LC) and C_f is the anatomical coordinate system of the femur. B) C_f was defined as follows: the origin was the midpoint between the medial collateral ligament (MCL) and lateral collateral ligament (LCL) insertions; the z-axis was made to pass through LCL and MCL (transepicondylar axis) and pointed towards the latter point. The y axis was defined as lying on the plane defined by LCL, MCL, and the centroid of the bone section (frontal plane) and perpendicular to the z axis pointing toward the proximal part of the bone. Finally, the x-axis was defined to be perpendicular to both the y- and the z-axes and oriented to generate a right-handed frame.

Fig. 2 The absolute error for the intact knee between displacements (A) and rotations (B) measured and computed with the compliance matrix at 30° of F-E is displayed. The values of A-P, P-D and M-L computed displacements (C) and measured forces (E), of A-A, I-E and F-E rotations (D) and moments (F) are also illustrated.

Fig. 3 Compliance matrix validation of the ACL-deficient knee. See Figure 2 for the explanation.

Table Caption List

Table 1 The experimental procedure for the compliance matrices calculation and validation is summarized in a chronological order

Table 2 Compliance matrix computed at 0° of F-E. Units of measurements are N, mm and rad. All the compliance matrix terms have to be scaled down by a factor of 10 $^{(-5)}$. In this and the following tables, F_x, F_y, F_z, M_x, M_y, M_z refer to the force and moment components, respectively, and T_x, T_y, T_z, R_x, R_y, R_z to the linear displacement components and the rotations, respectively.

Table 3 Compliance matrix computed at 30° of F-E. Units of measurements are N, mm and rad. All the compliance matrix terms have to be scaled down by a factor of 10 $^{(-5)}$.

Table 4 Compliance matrix computed at 15° and 45° of F-E. Units of measurements are N, mm and rad. All the compliance matrix terms have to be scaled down by a factor of 10 $^{(-5)}$.

Table 5 Compliance matrix computed at 60°, 75° and 90° of F-E. Units of measurements are N, mm and rad. All the compliance matrix terms have to be scaled down by a factor of 10 $^{(-5)}$.

Figure 1

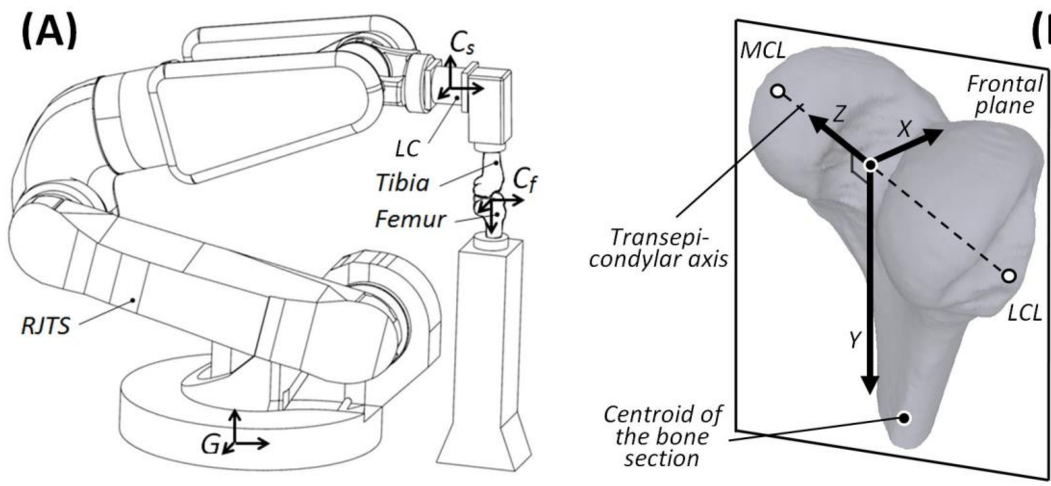
(A)
C_s
LC
Tibia
C_f
Femur
RJTS
G
(B)
MCL
Frontal plane
Z
X
Transepi-condylar axis
LCL
Y
Centroid of the bone section

Figure 2

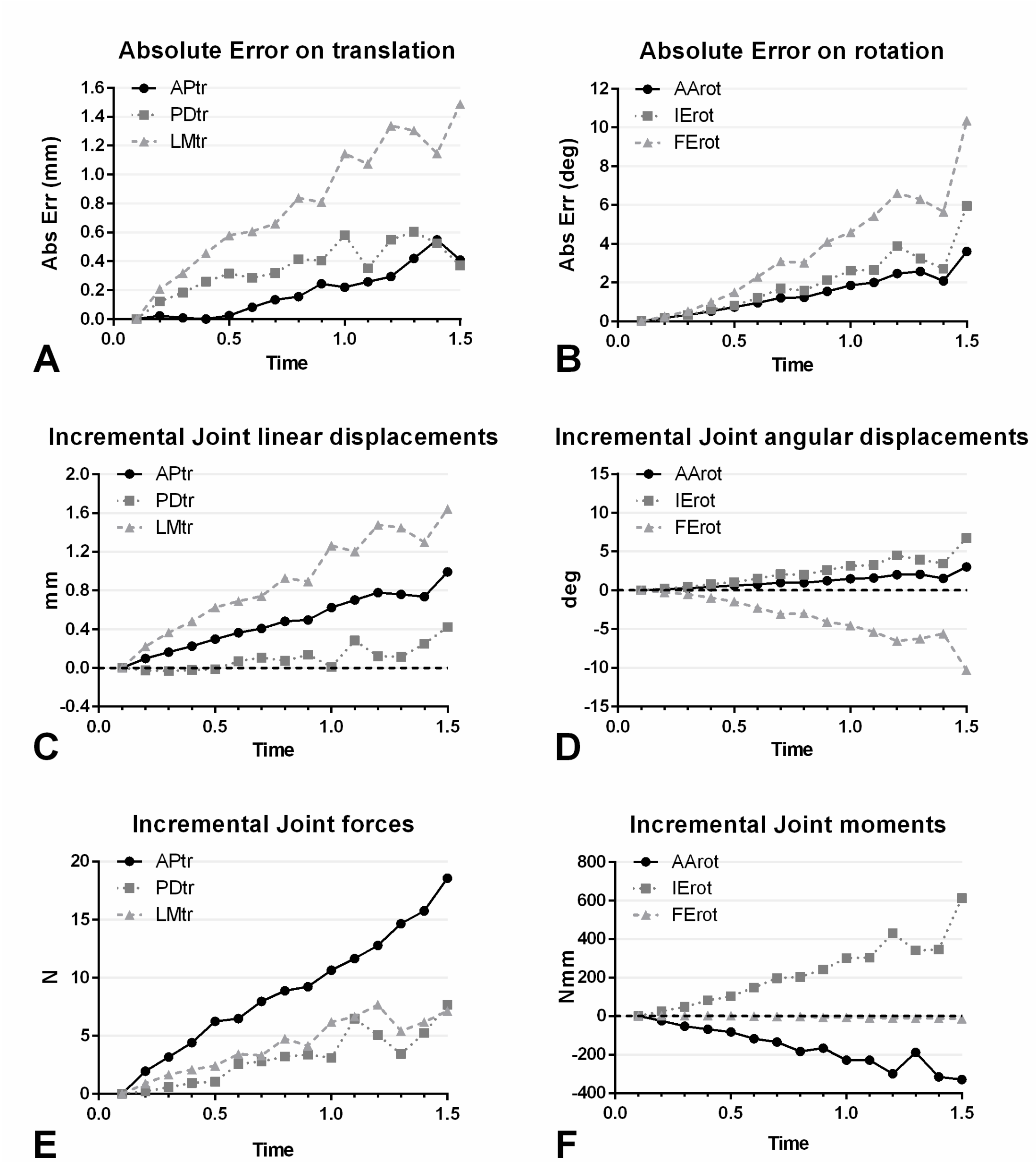
Absolute Error on translation
Abs Err (mm)
APtr
PDtr
LMtr
Time
A
Absolute Error on rotation
Abs Err (deg)
AArot
IErot
FErot
Time
B
Incremental Joint linear displacements
mm
APtr
PDtr
LMtr
Time
C
Incremental Joint angular displacements
deg
AArot
IErot
FErot
Time
D
Incremental Joint forces
N
APtr
PDtr
LMtr
Time
E
Incremental Joint moments
Nmm
AArot
IErot
FErot
Time
F

Figure 3

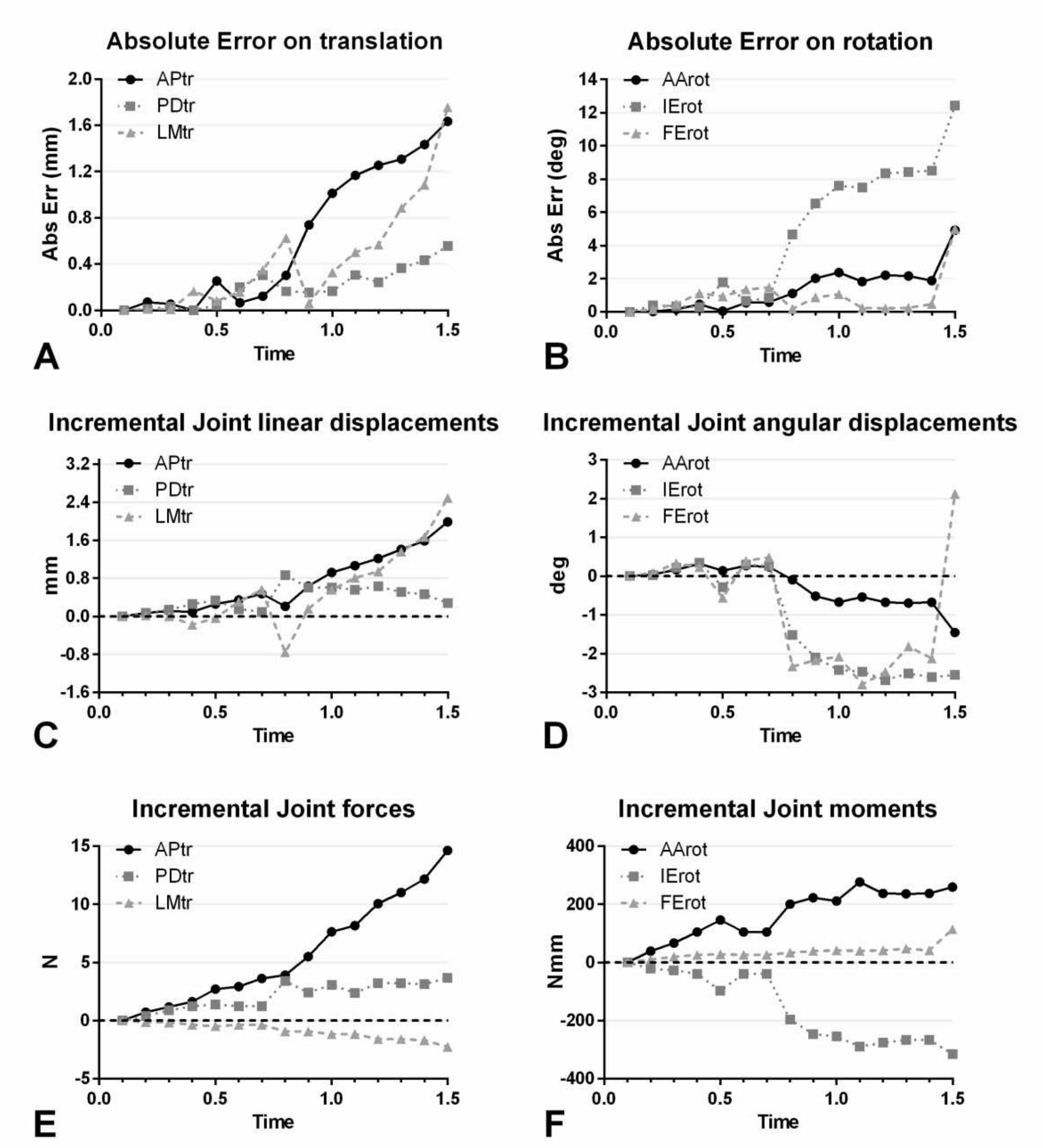
Absolute Error on translation
Abs Err (mm)
Time
APtr
PDtr
LMtr
A
Absolute Error on rotation
Abs Err (deg)
Time
AArot
IErot
FErot
B
Incremental Joint linear displacements
mm
Time
APtr
PDtr
LMtr
C
Incremental Joint angular displacements
deg
Time
AArot
IErot
FErot
D
Incremental Joint forces
N
Time
APtr
PDtr
LMtr
E
Incremental Joint moments
Nmm
Time
AArot
IErot
FErot
F

Table 1

Status of Knee	Knee F-E angle	Procedure steps	Robot Control	Compliance matrix calculation	Compliance matrix validation
Intact knee	0°, 15°, 30°, 45° 60°, 75° and 90°	Determination of neutral pose of the knee	Hybrid control	✓	
		Single DoF tests	Constrained Control	✓	
	30°	Lachman test	Force control		✓
ACL-deficient knee	0°, 15°, 30°, 45°, 60°, 75° and 90°	Single DoF tests	Constrained Control	✓	
	30°	Lachman test	Force control		✓

Table 2

Status of knee	F_x	F_y	F_z	M_x	M_y	M_z	
intact	8483.0	-3601.3	1653.0	24.7	113.1	185.0	T_x
ACL cut	*29173.0*	*-12305.8*	*-11451.1*	*104.8*	*-40.8*	*496.7*	
intact		5575.4	-561.1	-1.9	-43.4	-134.7	T_y
ACL cut		*14879.4*	*1225.2*	*59.2*	*15.0*	*-362.8*	
intact			15712.5	28.0	279.9	-135.9	T_z
ACL cut			*24440.1*	*-153.7*	*-66.0*	*-365.2*	
intact				3.4	2.7	1.3	R_x
ACL cut		Symmetric		*8.0*	*-1.3*	*-0.6*	
intact					11.7	2.5	R_y
ACL cut					*1.1*	*-0.8*	
intact						12.7	R_z
ACL cut						*22.0*	

Table 3

Status of knee	**F_x**	**F_y**	**F_z**	**M_x**	**M_y**	**M_z**	
intact	2991.3	572.9	5793.4	92.5	42.1	-180.0	**T_x**
ACL cut	*21321.8*	*-5513.2*	*27461.0*	*0.1*	*-332.5*	*-286.9*	
intact		8559.8	-5852.4	-7.6	1.6	-312.3	**T_y**
ACL cut		*17246.3*	*-24766.5*	*89.5*	*26.4*	*-258.2*	
intact			16999.8	190.3	68.3	-56.0	**T_z**
ACL cut			*76015.9*	*-217.6*	*-46.0*	*800.0*	
intact				9.8	8.5	-18.4	**R_x**
ACL cut		Symmetric		*33.9*	*39.1*	*-60.7*	
intact					21.2	-26.3	**R_y**
ACL cut					*62.9*	*-51.9*	
intact						126.7	**R_z**
ACL cut						*133.2*	

Table 4

15° of F-E

Status of knee	F_x	F_y	F_z	M_x	M_y	M_z	
Intact	15023.3	-14374.5	26922.1	-84.1	300.0	56.8	**T_x**
ACL cut	*44335.6*	*-313.0*	*-2912.9*	*-19.7*	*-808.2*	*-797.4*	
Intact		28838.7	-4517.2	293.0	128.1	-165.0	**T_y**
ACL cut		*13218.2*	*-6324.4*	*140.5*	*-135.7*	*-713.0*	
intact			96628.6	-175.2	-1065.2	108.3	**T_z**
ACL cut			*13028.0*	*-134.9*	*14.7*	*-227.9*	
intact				47.1	34.2	-16.6	**R_x**
ACL cut		Symmetric		*4.9*	*1.5*	*-4.6*	
intact					279.4	-13.7	**R_y**
ACL cut					*21.9*	*26.3*	
intact						26.5	**R_z**
ACL cut						*95.1*	

45° of F-E

Status of knee	F_x	F_y	F_z	M_x	M_y	M_z	
intact	2809.7	-2269.2	2404.2	80.8	131.0	-146.6	**T_x**
ACL cut	*6844.2*	*-2180.9*	*3974.5*	*7.5*	*-91.2*	*-183.7*	
intact		5999.5	-2814.8	-44.4	-233.3	-259.5	**T_y**
ACL cut		*6825.3*	*-3309.0*	*14.7*	*-173.7*	*-497.3*	
intact			5413.3	-38.9	-31.5	106.3	**T_z**
ACL cut			*8286.1*	*-15.4*	*-85.7*	*29.4*	
intact				6.1	7.7	-11.5	**R_x**
ACL cut		Symmetric		*3.7*	*0.3*	*-3.6*	
intact					25.3	-1.0	**R_y**
ACL cut					*18.2*	*28.0*	
intact						50.2	**R_z**
ACL cut						*62.2*	

Table 5

60° of F-E

Status of knee	F_x	F_y	F_z	M_x	M_y	M_z	
intact	1038.8	-2009.0	883.6	36.7	51.2	-19.6	T_x
ACL cut	*7395.4*	*390.6*	*7797.7*	*14.4*	*-335.8*	*-469.8*	
intact		4572.4	-614.6	-12.9	-70.6	-152.1	T_y
ACL cut		*13138.0*	*-16450.8*	*80.1*	*-163.3*	*-403.5*	
intact			6649.7	-129.9	-230.8	23.3	T_z
ACL cut			*54978.5*	*-37.2*	*-217.4*	*-328.3*	
intact				22.5	23.7	-37.3	R_x
ACL cut		Symmetric		*33.2*	*10.9*	*-27.6*	
intact					28.3	-35.1	R_y
ACL cut					*38.6*	*11.3*	
intact						81.5	R_z
ACL cut						*64.2*	

75° of F-E

Status of knee	F_x	F_y	F_z	M_x	M_y	M_z	
intact	4169.3	-3777.8	-605.7	9.7	26.8	107.9	T_x
ACL cut	*1957.1*	*-2342.8*	*457.9*	*6.8*	*-7.9*	*30.4*	
intact		3463.6	32.0	-0.1	-11.6	-99.6	T_y
ACL cut		*2841.6*	*-579.5*	*4.9*	*-5.8*	*-89.2*	
intact			6728.5	-104.2	-167.2	-20.3	T_z
ACL cut			*7293.1*	*-68.4*	*-161.7*	*-44.8*	
intact				3.3	3.8	-2.1	R_x
ACL cut		Symmetric		*8.7*	*-2.5*	*-17.0*	
intact					8.6	2.7	R_y
ACL cut					*13.2*	*23.8*	
intact						13.8	R_z
ACL cut						*77.2*	

90° of F-E

Status of knee	F_x	F_y	F_z	M_x	M_y	M_z	
intact	5369.0	-4264.1	84.9	-5.0	62.9	186.8	T_x
ACL cut	*3212.3*	*-2740.7*	*123.7*	*5.9*	*-66.1*	*10.8*	
intact		3668.6	-1475.8	18.5	-43.0	-156.1	T_y
ACL cut		*2784.9*	*-1602.1*	*24.1*	*-35.7*	*-158.0*	
intact			7038.5	-73.3	-40.4	35.5	T_z
ACL cut			*8908.0*	*-60.5*	*-133.3*	*-45.3*	
intact				1.9	1.5	0.4	R_x
ACL cut		Symmetric		*7.5*	*-10.2*	*-14.3*	
intact					10.7	11.0	R_y
ACL cut					*70.1*	*92.1*	
intact						15.5	R_z
ACL cut						*126.1*	